A Simulation Model for Predicting the Performance of a Built-in-Storage Solar Water Heater

Pachern Jansa, Supachart Chungpaibulpatana, and Bundit Limmeechokchai
Sirindhorn International Institute of Technology, Thammasat University,
P.O.Box 22, Thammasat Rangsit Post Office, Klong Luang, Patum Thani 12121, Thailand
Phone: (+662) 986-9009 ext. 3340, 2207, and 2206. Fax: (+662) 986-9009 ext. 1801
Email: p_jansa@hotmail.com, supachar@siit.tu.ac.th, and bundit@siit.tu.ac.th

Abstract

This paper describes a simulation model for predicting the thermal performance of a built-in-storage (BIS) solar water heater. The model has been developed based on the energy balances on three main components: absorber plate, collector channel and storage tank. The thermosyphon flow rate of water in the system has also been modeled and an overall flow coefficient K_f is introduced in the flow model as a system performance parameter, which must be determined from experimental tests on the system. A procedure to determine the values of K_f has also been established. Good agreement has been obtained from the comparison between the system thermal performance results predicted by the simulation model and those observed from the experimental tests conducted on the constructed BIS system. The BIS system performance parameters can be predicted by the developed model with errors of not more than 12 % for most sky conditions except very overcast sky. It is hoped that the developed simulation model can be used as a tool for analyzing the thermal performance of BIS solar water heaters and for further development in sizing the BIS system to meet the load requirements at any specific sites provided that their meteorological data are available.

Keywords: - Solar water heater; Built-in-storage; Thermosyphon; Thermal diode; Overall flow coefficient; System modeling; Simulation.

1. Introduction

Solar energy that is clean and abundant is among one of many alternative energy sources. It is widely exploited for useful energy in the form of heat and electricity. In the case of heating, solar water heaters have been investigated for many years. Most of them fall into two categories: (a) collection and storage in separate units and (b) collection and storage in the same unit. They can also be classified by different operations; active and passive systems. The active system operates with forced circulation by using an electric pump. The passive system operates with natural circulation and is often called the thermosyphon system. The collection and storage in separate units is considered as the conventional type of solar water heater since it has been used for a long time and is still widely used. The collection and storage in the same unit has recently received great interest due to its lower initial cost and simplified construction. It is known in several names such as a built-in-storage (BIS) type solar water heater, an integrated-collector- storage type solar water heater, an integral compact solar water heater, a collection-cum-storage solar water heater, or sometimes a low cost solar water heater. The system mainly consists of an inclined tank, in which the walls of the tank are thermally insulated, except the front wall, which is painted with black matte on the outside and covered with glass [6]. Different developments are suggested by researchers to improve the performance of the BIS so lar water heater, such as using an insulation cover during night-time [5] and using a transparent insulation [1]. Another modification of BIS solar water heater which utilizes a reflector to minimize radiation losses is also used [2]. The BIS solar water heater with a baffle plate placed between collector and storage tank is also proposed to reduce heat losses passed through the aperture area [4]. For a problem of convection losses during the night, a light plastic as a thermal diode is used to fix on an insulated baffle plate of a trapezoidal cross section tank to prevent reverse circulation [3].

As far as manufacturing is concerned, the trapezoidal cross section tank might be difficult to construct. Also, a light plastic plate used as a thermal diode might not be durable and not easy to change when damaged. A simple rectangular tank with a commercial check-valve as a thermal diode was therefore designed and constructed in order to conduct experimental tests. It has been shown that the constructed BIS system with a check-valve can reduce the night heat losses and its thermal efficiency was also found to be comparable to that of a conventional solar water heater tested simultaneously [11].

The thermal performance of the BIS solar water heater depends upon several factors, such as physical properties of various components as well as their sizes and configurations. To determine the effects of those components on the efficiency of the system, especially when it is operated under varying meteorological conditions, a simulation model is more preferred than actual constructions of several systems with different characteristics.

Thus, the main purpose of this study is to develop a simulation model for predicting the thermal performance of the constructed BIS solar water heater under varying weather conditions of solar irradiance, ambient temperature and wind speed. To verify the developed BIS system simulation model, the predicted results from the simulation are compared with those obtained from the experimental tests.

2. Configuration of the BIS solar water heater

Figure 1 shows the constructed BIS solar water heater. It consists of a solar absorber plate of 2.01-m^2 area which is integrated into a rectangular storage tank of 273-liter capacity. It is placed facing south with a tilt angle of 15°. The rectangular tank is made of stainless steel sheets. A corrugated absorber plate is made of a copper sheet which is painted with black matte. It is fixed over the tank and then covered by a 3-mm glass sheet. An air gap of 30 mm is left between the glass sheet and absorber plate. The sides and bottom of the tank is thermally insulated with 50-mm thick glass-fiber boards. An insulated partition is fixed between the absorber and storage tank. The partition is made of stainless steel sheets covering over a 25-mm thick styrofoam board. The gap between the absorber plate and insulated partition forms a collector channel of 25 mm in depth for a water flowing passage. At the lower and upper ends of the partition, a hole of 25-mm diameter is provided for water circulation between the collector channel and the tank. A commercial check-valve, the compressing spring of which is removed, is fixed to the hole at the lower end of the insulated partition. The valve is arranged so that it allows the water to flow only from the storage tank to the collector channel, whereas the reversed flow is prevented. This arrangement forms a thermal diode. When the water in the collector channel (between the absorber and insulated partition) is heated in the daytime, its density decreases. A pressure difference is built up between the storage tank and the collector channel. It lifts the valve lid to open and the cooler water flows out from the tank to the collector for solar heating. During the night the water in the collector channel cools down, and a pressure difference is established between the warm water in the storage tank and the cold water in the collector channel causing the valve lid to be closed thus preventing cold water to flow from the collector channel to the storage tank. For the purpose of investigation, tiny strings are attached to the lid of the check-valve so that it can be closed or opened by pulling the other ends of the strings through the vent hole. The temperatures of the water in both solar water heaters are measured by k-type thermocouples as shown in Fig 2. The ambient air temperature is also measured by a thermocouple. A pyranometer is used to measure the total solar irradiance on the collector surface. Wind speed around the test area is measured by a wind anemometer. A data logger is used to collect and record the data every 10 minutes.

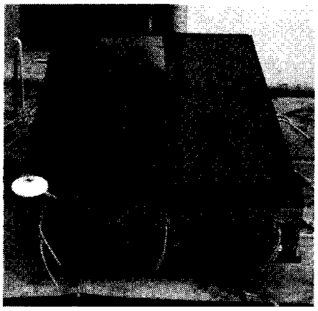

Fig. 1 The built-in-storage solar water heater.

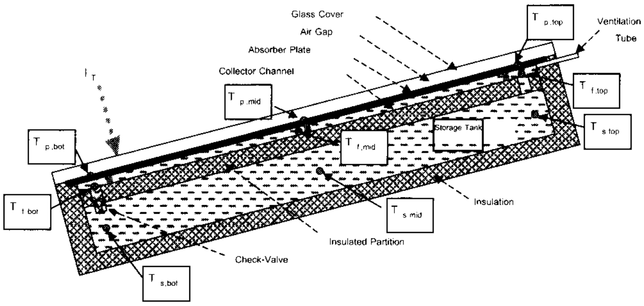

Fig. 2 Location of temperature measurements of the built-in-storage solar water heater.

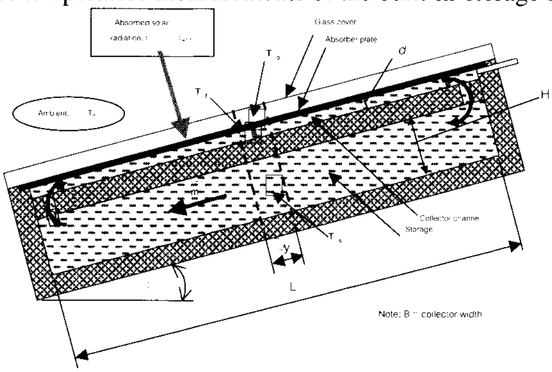

(a) Schematic diagram of the three main components and the position of temperature measurement

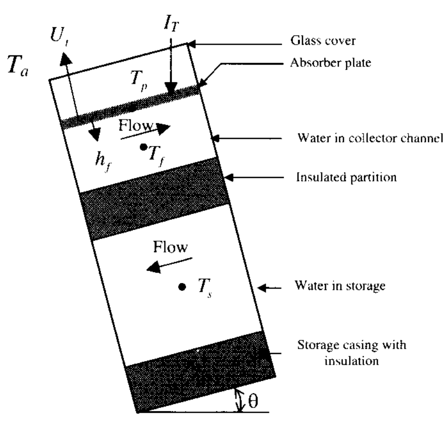

(b) Enlarged schematic diagram of the three main components for an elementary portion Δy

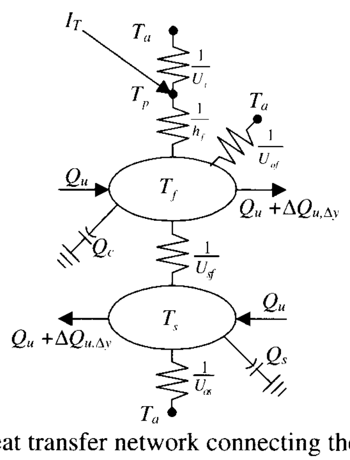

(c) Heat transfer network connecting the three main components

Fig. 3 Main components of the built-in-storage solar water heater for model formulation.

3. Mathematical Model Formulation

The thermal performance of the developed built-in-storage solar water heater can be described by the energy balances on three main components, i.e. the absorber plate, the water in the collector channel and the water in the storage tank as shown in Fig. 3.

Various assumptions are made in order to simplify the thermal analysis of the system based on the three main components. They can be explained as in the following.

1. The temperatures of the absorber plate, water inside the collector channel, and water inside the storage are represented by T_p, T_f and T_s respectively.
2. The heat capacities of the glass cover and the absorber plate are very small and negligible in comparison with that of water either in the collector channel or in storage.
3. The heat capacities of metal casing of insulated partition and metal distributor plates are very small, hence the heat capacity of the water in the collector channel is represented by that of the water inside the collector channel which is assumed to be at T_f. Similarly, for storage, the heat capacity of the storage is assumed to be that of the water inside the storage which is assumed to be at T_s.
4. The water mass flow rate is assumed to be uniform throughout the system.
5. Thermophysical properties (i.e. absorbtivity, emissivity and thermal conductivity) of materials (i.e. glass cover, absorber plate, metal wall and insulation) are constant and not a function of temperature.
6. The convective heat coefficient between the absorber plate and the water in the collector channel is assumed to be average for each portion.
7. Thermophysical properties (density, viscosity, specific heat, heat conductivity and thermal expansion coefficient) of water in the collector channel and in the storage tank vary with their respective water temperatures.

Based on the above assumptions, the three governing equations for an elementary portion Δy as shown in Figs. 3(a) and 3(b), on the absorber plate, the water in collector channel and in storage tank can be developed for characterizing the thermal performance of the built-in-storage solar water heater operated under the specified input conditions of solar irradiance, ambient temperature and wind speed as follows:

3.1 Absorber Plate

The energy balance on the absorber plate, the heat capacity of which is assumed to be negligible, can be described by:

$$Q_A - Q_{TL} = Q_{p-c} \qquad \text{or}$$

$$(\tau\alpha)_e I_T - U_t(T_p - T_a) = h_f(T_p - T_f) \qquad (1)$$

where Q_A = absorbed total solar radiation on the absorber plate (W/m^2), Q_{TL} = total heat losses from the top of the absorber plate to the ambient air (W/m^2), $Q_{p\text{-}c}$ = total heat transfer from the absorber plate to the water in collector channel (W/m^2), $(\tau\alpha)_e$ = effective transmittance-absorptance product of the collector, I_T = total solar irradiance falling on the collector surface (W/m^2), U_t = overall top loss coefficient between the absorber plate and ambient temperature taking into account the effect of glass cover (W/m^{2}K), T_p = average temperature of the absorber plate (°C), T_a = ambient temperature (°C), h_f = convective heat transfer coefficient between the absorber and water in the channel (W/m^{2}K), and T_f = average temperature of water in the channel (°C). From eq. (1), one gets:

$$T_p = \frac{(\tau\alpha)_e I_t + h_f T_f + U_t T_a}{h_f + U_t} \qquad (2)$$

The effective transmittance-absorbtance product can be approximated by:

$$(\tau\alpha)_e = 1.01\, \tau_g \alpha_p \qquad (3)$$

where τ_g = transmittance of glass cover, and α_p = absorptance of absorber plate.

The overall top loss coefficient can be calculated by the following equation.

$$U_t = \left[\frac{N}{\frac{C}{T_p^*}\left(\frac{T_p^* - T_a^*}{N+f}\right)^e} + \frac{1}{h_v} \right]^{-1} + \frac{\sigma(T_p^* + T_a^*)(T_p^{*2} + T_a^{*2})}{(\varepsilon_p + 0.00591 N h_v)^{-1} + \frac{2N + f - 1 + 0.133\varepsilon_p}{\varepsilon_g} - N} \qquad (4)$$

where N = number of glass cover, T_p^* = absolute absorber plate temperature (K), T_a^* = absolute ambient temperature (K), ε_g = emittance of glass cover, ε_p = emittance of absorber plate, σ = Stefan-Boltzmann constant (5.6697 x 10^{-8} W/m^{2}K^4), h_v = wind heat transfer coefficient = 5.7 + 3.8v_{wind} (W/m^2°C, where v_{wind} = wind speed across the front cover of the collector, (m/s)), $e = 0.43(1\text{-}100/T_p^*)$, $f = (1 + 0.089h_v - 0.1166h_v\varepsilon_p)(1 + 0.07866N)$, and $C = 520(1-0.000051\theta^2)$ for 0° < θ < 70°, θ = collector tilt angle (degree). Note that U_t is calculated based on projected area of the absorber plate. The equations (3) and (4) can be found in [7] and [8].

The convective heat transfer coefficient between the absorber and water in the collector channel can be calculated for the inclined plate facing downward with approximately constant heat flux as follows [9]:

$$h_f = \overline{Nu_e}\, k_w/\Delta y \qquad (5)$$

where $\overline{Nu_e}$ = average Nusselt number = $0.56(\mathrm{Gr_e\,Pr_e}\cos\theta)^{1/4}$ θ < 88°; $10^5 < \mathrm{Gr_e\,Pr_e}\cos\theta < 10^{11}$, $\mathrm{Gr_e} = g\rho\beta(T_p - T_f)L^3/\mu$, g = gravitational constant (m/s^2), ρ = density of water (kg/m^3), β = thermal expansion coefficient of water (K^{-1}), μ = viscosity of water (kg/m-s), k_w = thermal conductivity of water (W/mK), Δy = length of the portion (m). Note that all properties of water except β, used to calculated the average Nusselt number, are evaluated at a reference temperature $T_{ref1} = T_p - 0.25(T_p - T_f)$; β is evaluated at a temperature of $T_{ref2} = T_f + 0.5(T_p - T_f)$.

3.2 Collector Channel

The energy balance of the water in the collector channel for each portion dy at any instant is described by the following equation.

$$Q_c = Q_{p-c} - Q_{c-s} - Q_{c-a} - Q_u \qquad \text{or}$$

$$\rho_f d C_{pf}\frac{dT_f}{dt} = h_f(T_p - T_f) - U_{sf}(T_f - T_s) - U_{of}\left(\frac{2d}{B}\right)(T_f - T_a) - \frac{\dot{m}C_{pf}}{B}\frac{dT_f}{dy} \qquad (6)$$

where Q_c = total energy stored in the water in the collector channel at any instant (W/m^2), Q_{c-s} = energy transfer between water in the collector channel and the storage tank by passing through the insulated partition (W/m^2), Q_{c-a} = energy loss from the collector channel to the ambient air (W/m^2), Q_u = useful energy in the water flowing out from the collector channel (W/m^2), ρ_f = density of the water in the collector channel (kg/m^3), d = collector channel depth (m), B = width of collector channel (m), C_{pf} = specific heat of water in the collector channel (kJ/kgK), $\dot{m}$ = mass flow rate of water flowing through the system (kg/s), T_f = water temperature in the collector channel (°C), T_s = water temperature in the storage tank (°C), and U_{sf} = heat transfer coefficient between water in the channel and the storage tank (W/m^{2}K) = k_{sf}/l_{sf}, where k_{sf} = heat conductivity of the insulated partition and l_{sf} = thickness of the insulated partition, U_{of} = heat losses coefficient from water in the collector channel through the side insulation wall to the ambient air (W/m^{2}K) = k_{of}/l_{of}, where k_{of} = heat conductivity of the wall insulation partition and l_{of} = thickness of the wall insulation. After substituting an expression of T_p into eq. (6) one has:

$$\rho_f d C_{pf}\frac{dT_f}{dt} = \frac{h_f[(\tau\alpha)_e I_T - U_t(T_f - T_a)]}{h_f + U_t} - U_{sf}(T_f - T_s) - U_{of}\left(\frac{2d}{B}\right)(T_f - T_a) - \frac{\dot{m}C_{pf}}{B}\frac{dT_f}{dy} \qquad (7)$$

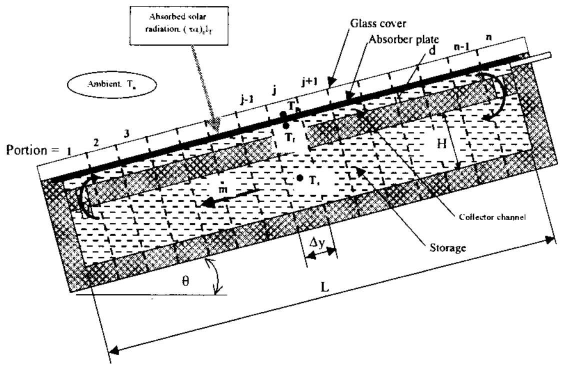

Fig. 4 Schematic diagram of the system divided into n equal portions.

Since the partial differential form of eq. (7) is not easy to solve analytically, a finite difference numerical method is used. If the collector channel is represented by n portions along its flow direction as shown in Fig. 4. The temperature of the j^{th} portion at the next time step Δt can be written as follows:

$$T_{f_j}^{t+\Delta t} = T_{f_j}^{t} + \frac{\Delta t}{\rho_f^t d C_{pf}^t}\Big\{\frac{h_f^t[(\tau\alpha)_e I_T^t - U_t^t(T_{f_j}^t - T_a^t)]}{h_f^t + U_t^t} - U_{sf}(T_{f_j}^t - T_{s_j}^t) - U_{of}\Big(\frac{2d}{B}\Big)(T_{f_j}^t - T_a^t) - \frac{\dot{m}^t C_{pf}^t}{B\Delta y}(T_{f_j}^t - T_{f_{j-1}}^t)\Big\} \quad (8)$$

where T_f^t = water temperature in the collector channel at time t (°C), $T_f^{t+\Delta t}$ = water temperature in the collector channel at time $t+\Delta t$ (°C), T_s^t = water temperature in the storage tank at time t (°C), T_a^t = ambient temperature at time t (°C), ρ_f^t = density of the water in the collector channel at time t (kg/m^3), C_{pf}^t = specific heat of water in the collector channel at time t (kJ/kgK), I_T^t = total solar irradiance falling on the collector surface at time t (W/m^2), h_f^t = convection heat transfer coefficient between the absorber and water in the channel at time t (W/m^{2}K), U_t^t = overall top loss coefficient between the absorber plate and ambient temperature taking into account the effect of glass cover at time t (W/m^{2}K), and $\dot{m}^t$ = mass flow rate of water flowing through the system at time t (kg/s).

Note that, for the bottom and the top end portions of the collector channel, there is an additional heat loss from the water through the end side to the ambient air. Hence the 3rd heat loss term on the right hand side of eq. (8) must be replaced by $U_{of}(1/\Delta y + 2/B)d(T_{f_j}^t - T_a^t)$.

3.3 Storage Tank

The energy balance for an elementary portion dy of the water in the storage tank can be described by the following equation.

$$Q_s = Q_u + Q_{c-s} - Q_{s-a} \qquad \text{or}$$

$$\rho_s H C_{ps}\frac{dT_s}{dt} = \frac{\dot{m}C_{ps}}{B}\frac{dT_s}{dy} + U_{sf}(T_f - T_s) - U_{os}\Big(1 + \frac{2H}{B}\Big)(T_s - T_a) \quad (9)$$

where Q_s = total energy stored in the water in the storage at any instant (W/m^2), Q_{s-a} = energy loss from the storage to the ambient air (W/m^2), ρ_s = density of the water in the storage tank (kg/m^3), H = storage tank depth (m), C_{ps} = specific heat of water in the storage tank (kJ/kgK), U_{os} = heat loss coefficient between the storage tank and ambient (W/m^{2}K); $U_{os} = k_{os}/l_{os}$, where k_{os} = heat conductivity of tank wall insulation (W/mK) and l_{os} = thickness of tank wall insulation (m). If the tank is represented by n portions in the same way as the collector channel as shown in Fig. 4. The temperature at the next period of time for the j^{th} node can be written as:

$$T_{s_j}^{t+\Delta t} = T_{s_j}^{t} + \frac{\Delta t}{\rho_s^t H C_{ps}^t}\Big[\frac{\dot{m}^t C_{ps}^t}{B\Delta y_j}(T_{s_{j-1}}^t - T_{s_j}^t) + U_{sf}(T_{f_j}^t - T_{s_j}^t) - U_{os}\Big(1 + \frac{2H}{B}\Big)(T_{s_j}^t - T_a^t)\Big] \quad (10)$$

where $T_s^{t+\Delta t}$ = water temperature in the storage tank at time $t + \Delta t$ (°C), ρ_s^t = density of water in of storage tank at time t (kg/m^3), C_{ps}^t = specific heat of water in the storage tank at the time t (kJ/kgK). Note that, for the bottom and the top end portions of the storage, there is an additional heat loss from the water through the end side to the ambient air. Hence the 3rd heat loss term on the right hand side of eq. (10) must be replaced by $U_{os}(1 + 2H/B + H/\Delta y)(T_{s_j}^t - T_a^t)$.

3.4 Thermosyphon Flow Rate

a) Thermosyphon Head

The thermosyphon built-in-storage solar water heater and its density-head diagram can be shown in Fig. 5. The thermosyphon head at any instant is created by the difference between the total pressure head along the path 123 and that along the path 143.

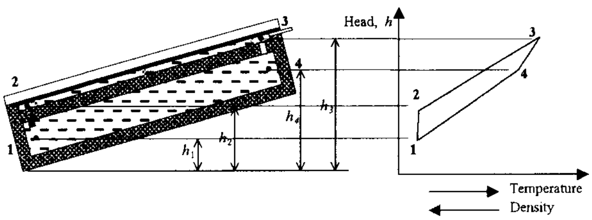

Fig. 5 The density head diagram of the system.

The thermosyphon head (H_T) can be described by:

$$\text{H}_\text{T} = \int_1^2 \rho g dh + \int_2^3 \rho g dh - \int_1^4 \rho g dh - \int_4^3 \rho g dh \quad (11)$$

where h = the vertical height (m). Since the temperature variation of water inside the system is small, the water temperature is assumed to be linearly dependent on its density i.e. $T = C\rho g$, where C is a constant. The thermosyphon head can then be expressed as:

$$\text{H}_\text{T} = C_1(h_2 - h_1)(T_{mb} - T_{sb}) + C_1(h_3 - h_2)(T_{fm} - T_{sb}) - C_1(h_2 - h_1)(T_{sm} - T_{sb}) - C_1(h_3 - h_4)(T_{mt} - T_{sb}) \quad (12)$$

where C_1 = constant, T_{fm} = average temperature of the water in the collector channel (°C), T_{sm} = average temperature of the water in the storage tank (°C), T_{mb} = average temperature of the water at the bottom, $(T_{sb}+T_{fb})/2$, (°C), T_{mt} = average temperature of the water at the top, $(T_{ft}+T_{st})/2$, (°C), T_{sb} = temperature of the water at the bottom of the storage (°C), T_{fb} = temperature of the water at the bottom of the collector channel (°C), T_{ft} = temperature of the water at the top of the collector channel (°C), T_{st} = temperature of the water at the top of the storage (°C).

b) Friction Head

The total friction head that occurs in the built-in-storage solar water heater due to the friction of water flowing through the entrance, exit, distributor and check valve in the flow circuit can be described by:

$$\text{H}_\text{F} = C_2 V^2 = C_3 \dot{m}^2 \quad (13)$$

where C_2, C_3 = constant, V = velocity of flow (m/s). Note that the friction due to the viscosity of water along the collector channel is relatively small in comparison with the above-mentioned friction. However it can be assumed that this small effect is already included in eq (13).

c) Mass Flow Rate

Equating eqs. (12) and (13), the mass flow rate in passing through the collector channel can be obtained as:

$$C_3\dot{m}^2 = C_1\{(h_2 - h_1)(T_{mb} - T_{sb}) + (h_3 - h_2)(T_{fm} - T_{sb}) - (h_4 - h_1)(T_{sm} - T_{sb}) - (h_3 - h_4)(T_{mt} - T_{sb})\} \quad (14)$$

or

$$\dot{m} = K_f\{(h_2 - h_1)(T_{mb} - T_{sb}) + (h_3 - h_2)(T_{fm} - T_{sb}) - (h_4 - h_1)(T_{sm} - T_{sb}) - (h_3 - h_4)(T_{fm} - T_{sb})\}^{(1/2)} \quad (15)$$

where K_f = the overall flow coefficient due to the friction along the water flow passage through distributor, inlet and outlet hole of the collector channel and check valve (kg $s^{-1}\{m\ K\}^{-1/2}$).

3.5 Thermal Performance Indicators

The useful energy is calculated based on heat stored in the storage tank as the following:

$$Q_u = M_s C_p (T_2 - T_1) \quad \text{(kJ)} \quad (16)$$

where M_s = mass capacity of water in the storage tank (kg), T_1 = average water temperature in the storage tank at sunrise (°C), T_2 = average water temperature in the storage tank at sunset (°C). The collection efficiency η_c during the day is defined as the ratio of amount of heat stored in the storage tank during the daytime to the energy absorbed by the collector as follows:

$$\eta_c = \frac{Q_u}{A_c G_T} \quad (17)$$

where G_T = total solar energy falling on the collector (kJ/m^2). The storage efficiency η_s during the cool-down period at night is determined based on the remaining heat content of the storage tank before sunrise of the next morning to the maximum possible heat losses from the storage tank as follow:

$$\eta_s = \frac{T_3 - T_{a,night}}{T_{s,\max} - T_{a,night}} \quad (18)$$

where T_3 = average water temperature in the storage tank before sunrise of the next morning (°C), $T_{s,max}$ = maximum average water temperature in the storage tank (°C), $T_{a,night}$ = average ambient temperature during the night (°C). The system efficiency during 24 hours η_{24hour} is defined as amount of heat stored in the storage before sunrise of the next morning to the energy falling on the collector as follows:

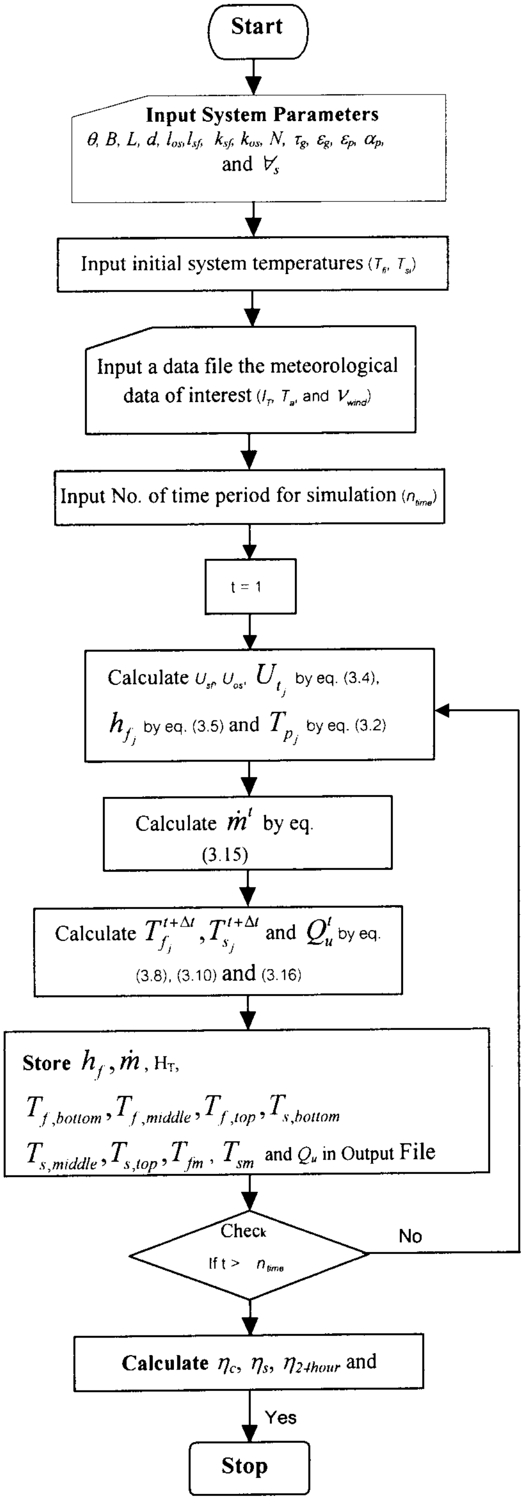

Fig. 6 Flow chart of simulation program.

$$\eta_{24hour} = \frac{M_s C_p (T_3 - T_1)}{A_c G_T} \qquad (19)$$

The amount of energy stored in the storage tank before sunrise of the next morning can be calculated as:

$$Q_{morning} = M_s C_p (T_3 - T_{a,morning}) \quad \text{(kJ)} \qquad (20)$$

where $T_{a,morning}$ = ambient temperature at the same time of T_3 (°C).

4. System Simulation Procedure

As mentioned earlier, a finite difference method has been used to solve the thermal performance of the constructed BIS system by dividing the system into several portions along the length of the system as shown in Fig. 4. For the simulation, the BIS system was divided into 17 portions along the length of the collector. The parameters of the system used in the simulation are listed in Table 1 and the simulation procedure can be described by Fig. 6.

Table 1 Parameters of the system used in the simulation.

Parameter	Value
Inclination angle of the system, θ	15° *
Latitude of test location, *Lat*	15° (north)
Collector width, B (m)	1.1 *
Collector length, L (m)	1.7 *
Average channel depth of the collector passage, d (m)	0.0425 *
Wall insulation thickness, l_{os} (m)	0.03 *
Insulated partition thickness, l_{sf} (m)	0.035 *
Wall insulation heat conductivity, k_{os} (W/mK)	0.07 **
Insulated partition heat conductivity, k_{sf} (W/mK)	0.15 **
Number of glass cover, N	1
Transmittance of glass cover, τ_g	0.88 **
Emittance of glass cover, ε_g	0.88 **
Emittance of absorber plate, ε_p	0.95 **
Absorptance of absorber plate, α_p	0.8 **
Water volume in storage tank, V_s (liters)	273 *
Heights ($h_2 - h_1$) and ($h_3 - h_4$) in Fig. 3.4 (m)	0.10*
Heights ($h_3 - h_2$) and ($h_4 - h_1$) in Fig. 3.4 (m)	0.46*

* Obtained from measurement
** Obtained from manufacturer's specifications

5. Determination of Overall Flow Coefficient, K_f

5.1 Determination procedure

Beside the parameters of the system given in Table 1, there is one more parameter, i.e. the overall flow coefficient K_f, which appears in eq. (15) and must be known so that the thermosyphon mass flow rate, $\dot{m}$, of the water circulating in the system can be predicted by the simulation. K_f is the overall effects of all frictions occurred along the water flowing passage throughout the system. K_f accounts for the frictions of the valve entrance and exit, the distributors, the walls in the collector channel and in the storage. It has been mentioned earlier that the average value of K_f is difficult to be theoretically determined from the physical properties and configurations of those components along the flow passage. It is suggested to determine K_f from experimental tests on the system. In the experiment, if the value of $\dot{m}$ could be measured accurately, the value of K_f would be determined directly using eq. (15) as other parameters in the system could be easily obtained by the measurements. Unfortunately it is not easy to measure the thermosyphon mass flow rate occurring in the constructed BIS solar water heater because the flow rate is very small.

Hence, a trial and error procedure is proposed to determine the value of K_f from the experimental data obtained from the tests on the system. Several values of K_f are guessed systematically and inputed to the simulation program. For each value of K_f, the program predicts the average temperature of the water in the storage tank, T_{sm}, at any time interval of interest in accordance with the given meteorological data observed from the experimental test. These simulated values of T_{sm} are compared with their corresponding values of T_{sm} observed from the experiment. Their errors are estimated and the standard errors of estimate (SEE) of T_{sm} is then calculated by:

$$\mathrm{SEE} = \left| \frac{\sqrt{\sum_{i=1}^{n}(T'_{sm,cal_i} - T'_{sm,\exp_i})^2}}{n-1} \right| (^\circ\mathrm{C}) \qquad (21)$$

where $T'_{sm,cal}$ = average temperature of the water in the storage resulting from simulation at any time t (°C), $T'_{sm,\exp}$ = average temperature of the water in the storage resulting from experiment at any time t (°C), n = number of data. Finally the value of K_f that produces the minimum value of SEE is therefore selected for the system under the considered condition.

The water in the collector channel flows upward during the heating period and, if a provision for preventing reverse thermosyphon flow is not installed in the system, the water would flow downward in the collector channel during the night or cooling down period. Hence the value of the overall flow coefficient K_f during the heating may differ from that during the cooling since different friction resistances can be expected from the opposite direction of flow through any passage. Hence K_f is considered from two parts of data of each experimental test run, i.e. K_f for the heating period and K_f for the cooling period. For the heating period, K_f is suggested to determined from the days with high solar radiation intensity, say about 20 MJ/m^2. Note that with such a high insolation day it is ascertained that the water flow exists in the system with a rate high enough to give accurate results of K_f.

The value of K_f for the heating period is determined using the experimental data over the period which the thermosyphon head, H_T, calculated by eq. (12) is found to be a positive value whereas K_f for the cooling period is determined from the period when the thermosyphon head is negative. As, in each test, the system cooling down period occurred in the evening after the daytime heating up period, K_f for the heating period is determined first and then the accepted value of K_f for the heating period will be used to determine K_f for the cooling period.

5.2 Determination Results

In experimental testing, the developed built-in-storage solar water heating system was tested for 24 hours starting from early morning at 06.00 hours under 3 cases of different operations of the check-valve installed in the flow passage. The three different operational cases can be described as follows:

Case 1: The check-valve in the flow passage was forced open throughout the test i.e. reverse circulation may occur at night.

Case 2: The check-valve was allowed to work freely throughout the test. The valve opening is dependent on the pressure difference between each side of the valve lid.

Case 3: The check-valve was allowed to work freely during the day but forced closed at night i.e. no reverse circulation at night may occur.

The best values of K_f obtained using the above mentioned determination procedure for both heating and cooling periods of several experimental test runs are shown in Table 2. For purpose of sample illustration of how the best value of K_f is selected, the plot of several values of K_f obtained for Case 2 on 15/11/2002 are presented in Fig 7. It is clearly seen that, for heating case, the minimum value of SEE of 0.08 °C (or about 0.2 % of the average value of T_{sm} of 40.0 °C) is found at $K_f = 0.00045$ kg s^{-1} (mK)$^{-1/2}$. Similarly, in the cooling period case, the value of SEE is minimum when $K_f = -0.0002$ kg s^{-1}.(mK)$^{-1/2}$. Note that the negative K_f means that the flow is in the reverse direction. The SEE is about 0.02 °C (or 0.05 % of the average value of $T_{sm} = 42.4$ °C) during the cooling period.

In Table 2, it is found that K_f for the heating period of Case 1 is higher than those of Case 2 and Case 3. As K_f is directly related with the mass flow rate of water circulating in the system, this means that the flow rate in Case 1 was higher than the other two cases. Note that with higher K_f, the resistance to flow is less, resulting in a higher flow rate. This can be explained by the fact that, in Case 1, the check-valve installed in the flow passage was forced to fully open throughout the day (and the night as well). The resistance to flow was therefore less than those of the other two cases in which the check-valve was allowed to work freely, i.e. the valve was usually partly opened depending on the driving force created by differential pressures of water located at both sides of the valve. The valve was then very rarely in the full opening position. Similar results were also found in the case of cooling at night in which relatively high reverse flow was shown in Case 1 in comparison with those in the other two cases. Note that, in Cased 3 in which the check-valve was forced closed, the value of K_f obtained from the night was not zero as it must be in reality. However the obtained value was very small and actually very close to zero. The small discrepancy may be explained by the errors in experimental measurements. It should also be noted here that the value of K_f for the night-time period was found to be quite low for Case 2, indicating that the installed check-valve could significantly stop the reverse circulation.

6. Simulation Results and Discussion

To validate the developed mathematical model in predicting the system performance under Case 2 which is the normal condition of check-valve in actual operation, the thermal performance parameters of the system such as T_{sm}, T_{fm}, η_c, η_s, η_{24hour} and $Q_{morning}$, simulated by the program described in section 3 were compared with those obtained from the experiments. The meteorological data, i.e. I_T, T_a, V_{wind}, recorded from several test runs under Case 2 were used as the inputs to the program along with the fixed system parameters given in Table 1. The values of overall flow coefficients K_f (for heating and cooling period) for Case 2 of check-valve operation shown in Table 2 were then taken for the simulation. A sample of the simulation results obtained for the test on the system under Case 2 on 15/11/2002 is shown in Fig.8.

It can be seen from the figure that there is good agreement between the values of $T_{sm,cal}$ obtained from the simulation and the values of $T_{sm,exp}$ observed from the experiment. The average deviation (i.e. the value of SEE) is about 0.03 °C or 0.07 % of the average value of T_{sm} of 40.6 °C throughout the test period. The simulation results obtained from other test runs are similarly illustrated. Their corresponding values of SEE between $T_{sm,cal}$ and $T_{sm,exp}$ are provided in Table 3. The results show that the model is able to simulate the mean storage temperatures of the system in good agreement with the experimental values. The maximum SEE found is about 0.12 °C on 11/10/2002. In Fig. 8, high values of $T_{fm,cal}$ estimated by the model can be seen during the heating period. The over estimations of $T_{fm,cal}$ may come from several factors. The property deteriorations of the collector components, such as glass cover, absorber plate and insulation, after several test runs might result in lower performance than that estimated by the simulation using their original properties taken from the manufacturers' specifications. The errors in estimating the overall flow coefficient K_f from the experimental data may also contribute some errors in determining the thermosyphon flow rate in the system which affects the prediction of $T_{fm,cal}$. Detailed investigations on these effects to improve the accuracy in simulating the value of T_{fm} should be carried out. However, all parameters for characterizing the thermal performance of the system in this study; those are η_c, η_s, η_{24hour} and $Q_{morning}$, are calculated using the temperature of water in the storage, T_{sm}, not that of water in the collector channel T_{fm}. Hence the developed model can be used to determine these system performance parameters with confidence. This can be confirmed by Table 3 which illustrates the simulated results of these parameters obtained from several test runs in comparison with those observed from the experiments. The percentage errors for all parameters in most test runs are found to be within ± 12 % except the test run under very low solar radiation (i.e. 17/8/2002).

Figure 9 illustrates the ability of the developed model in simulating the dynamic variations of system temperatures in response to the changes in solar irradiance, ambient temperature and wind velocity for three consecutive days. The system temperatures measured from the experiment conducted during these three days are also presented for comparison. Satisfactory agreement is shown in the prediction of the mean storage temperatures of the system, T_{sm}. But, for the values of the mean temperature of the water inside the collector channel, T_{fm}, although large deviations are found during the heating period, especially on sunny days, the simulated values vary following the trends observed from the experiment. However, as mentioned earlier, T_{fm}, does not affect the prediction of the performance of the system. It can be concluded here that the developed model can be used to determine the long-term performance of the BIS system if long-term meteorological data are available.

7. Conclusions

(a) A mathematical model has been formulated for simulating the transient thermal performance of the developed BIS solar water heater operated under varying weather conditions of solar irradiance, ambient temperature and wind speed. The model consists of the submodel for three components of the system, i.e. absorber plate collector channel and storage tank. Almost all performance characteristics for components in each submodel can be obtained from either manufacturers' specifications or direct measurements except the very slow thermosyphon flow, which is very difficult to measure accurately. Hence, a submodel for estimating the thermosyphon flow rate along the flow circuit between the collector channel and storage tank has also been proposed. An overall flow coefficient K_f has been introduced in the submodel to reflect the overall effects of various frictions occurring along the water flow passage. A procedure for determining the value of K_f from the experimental test conducted on the BIS system has been described. Finally a computer simulation package was written based on the developed model.

(b) Using experimental data obtained from various test runs on the BIS system under different operations of check-valve, the values of K_f determined according to the above-mentioned procedure have been successfully found to be consistent, that is a higher K_f which results in higher flow rate is obtained when the check-valve is forced fully open. Hence the overall flow coefficient K_f can be used as a performance parameter for the BIS system.

(c) The developed simulation model has been used to simulate the thermal performance of the constructed BIS system using the meteorological data obtained from the experimental tests as inputs to the computer program. It has been found from the comparisons that most system performance results predicted by the simulation model satisfactorily agree with these corresponding values observed from the experimental tests. The deviations found are within ± 12 %. Therefore it can be concluded that the developed simulation model can be used for analyzing the thermal performance of BIS solar water heating systems and for further development in sizing the system to meet the load requirements under the meteorological conditions at the site location.

8. Acknowledgements

Gratitude is extended to Sripatum University and the Energy Policy and Planning Office--EPPO (formally called the Thailand National Energy Policy Office--NEPO) for their kind contribution in providing partial financial support.

9. References

[1] M. Arulanantham, K. S. Reddy and N. D. Kaushika, Solar Gain Characteristics of Absorber Parallel Transparent Insulation Materials. Energy Conversion and Management Vol, 39, pp.1519-1527, 1998.

[2] G.N. Tiwari Doung Duc Hong and R.K. Goyal, A Low Cost Solar Water Heater Suitable for Rural, as Well as Urban, Areas

of Vietnam. Energy Conversion and Management Vol. 39, pp. 953-962, 1998.
[3] A.A. Mohamad, Integrated Solar Collector-Storage Tank System with Thermal Diode. Solar Energy, Vol. 61, pp. 211-218, 1997.
[4] I.N. Kaptan and A. Kilic, A Theoretical and Experimental Investigation of a Novel Built-in-storage Solar Water Heater. Solar Energy, Vol. 57, pp. 393-400, 1996.
[5] S.C. Kaushik, Rakesh Kumar, H.P. Garg, and J. Prakash, Transient Analysis of a Triangular Built-in-storage Solar Water Heater under Winter Conditions. Heat Recovery Systems & CHP, Vol. 14, pp. 337-341, 1994.
[6] M.S. Sodha, J.K. Nayak, S.C. Kaushik, S.P. Sabberwal, and M.A.S. Malik, Performance of a Collector/storage Solar Water Heater. Energy Conversion and Management, Vol. 19, pp. 41-47, 1979.
[7] John A. Duffie and William A. Beckman, Solar Engineering of Thermal Processes (First Edition). John Wiley & Sons, Inc, 1980.
[8] John A. Duffie and William A. Beckman, Solar Engineering of Thermal Processes (Second Edition). John Wiley & Sons, Inc, 1991.
[9] J. P. Holman, Heat Transfer. McGraw-Hill, Inc, 1997.
[10] G.Y. Saunier, Ph. Bouix, Supachart Chungpaibulpatana, and Thada Vitagsabootr, A Test Procedure for Thermosyphon Solar Water Heaters. Solar Thermal Component and System Testing: Proceedings of the Fourth Asian School on Solar Energy Harnessing 12-20 December 1985 at AIT, Bangkok, pp. 163-177, 1985.
[11] P. Jansa, S. Chungpaibulpatana, and B. Limmeechokchai, A Simple Built-in-Storage Solar Water Heater for Remote Areas, Proceedings of the 2nd Regional Conference on Energy Technology Towards a Clean Environment, The Joint Graduate School of Energy and Environment on 12-14 February 2003 at Phuket, Thailand, pp. 422-428, 2003.

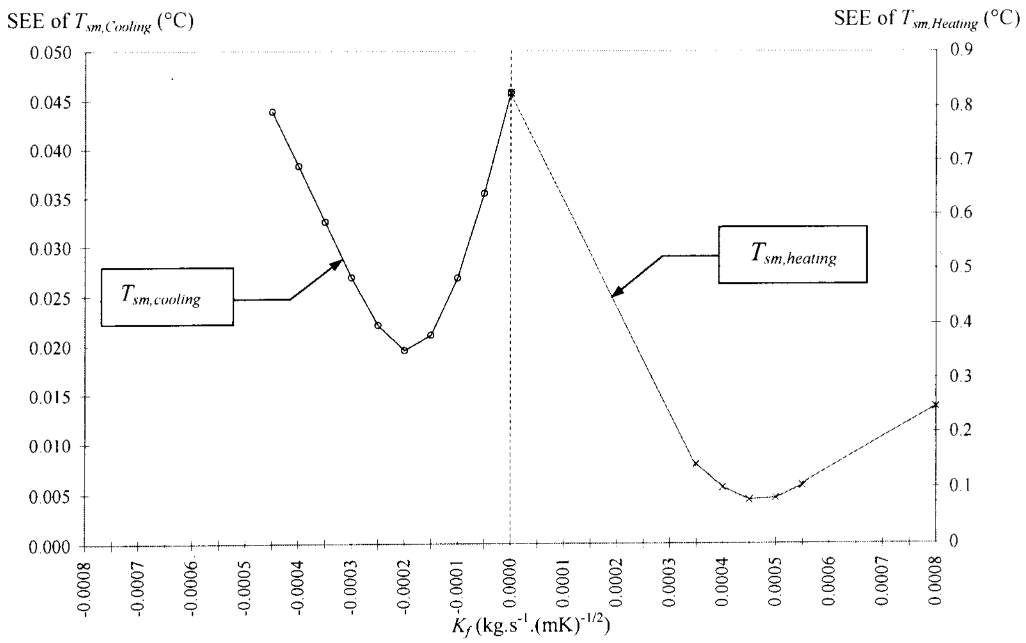

Fig. 7 Standard errors of estimate of T_{sm} found at different values of K_f.

Table. 2 Best values of the overall flow coefficient K_f obtained for three different operations of check-valve.

Operation of check-valve	Date of Experiment	I_T (MJ/m^2)	Heating Period		Cooling Period	
			Value of K_f (kg.s^{-1}.(mK)$^{-1/2}$)	SEE (°C)	Value of K_f (kg.s^{-1}.(mK)$^{-1/2}$)	SEE (°C)
Case 1: check-valve open throughout the test (reverse circulation at night)	9/10/2002	20.7	0.00150	0.18	-0.01550	0.10
Case 2: check-valve operated freely throughout the test	15/11/2002	20.7	0.00045	0.07	-0.00020	0.02
Case 3: check-valve operated freely during the day but closed at night (no reverse circulation at night)	12/7/2002	19.7	0.00060	0.08	-0.00025	0.15

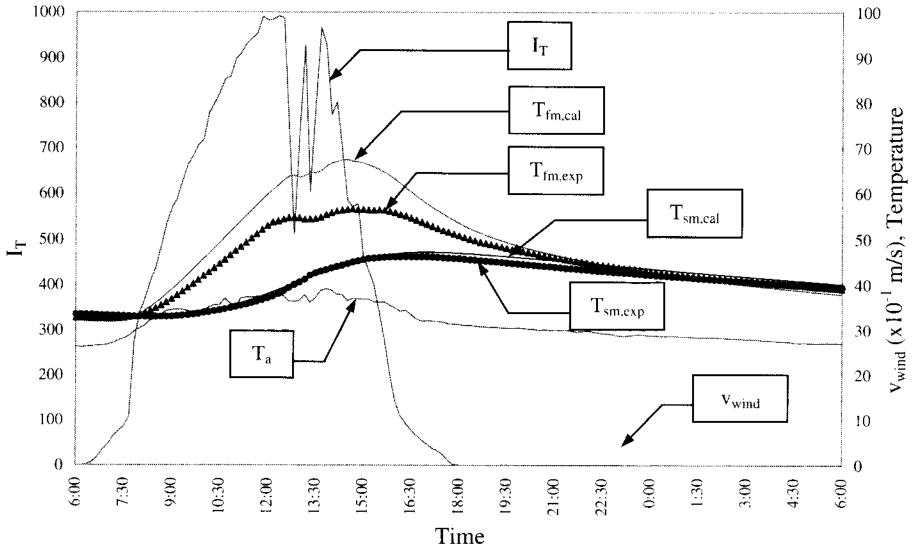

Fig.8 Simulation results in comparison with experimental results on 15/11/2002

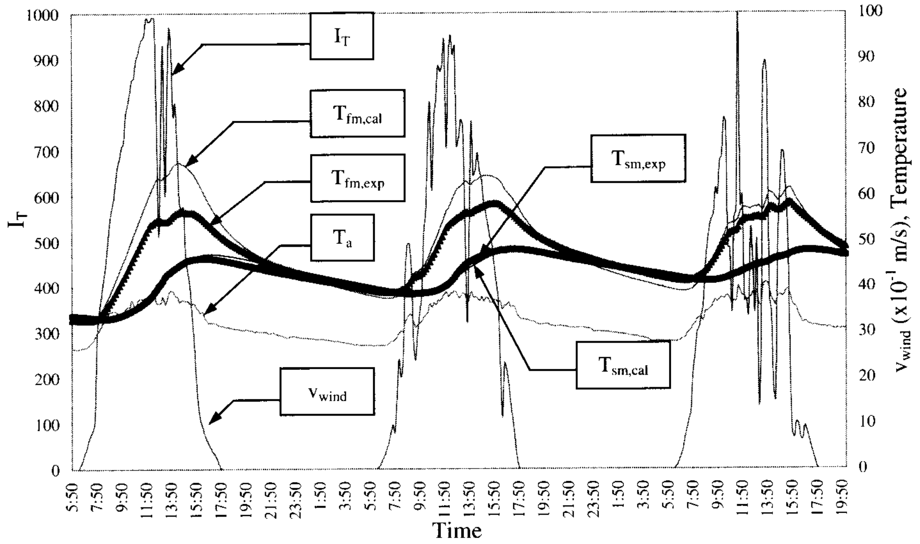

Fig. 9 Simulation results of three-consecutive-day in comparison with those obtained from experiments.

Table. 3 Thermal performances of the BIS system resulting from simulation and experiment when the check-valve operated freely through the test.

Date	I_T (MJ/m^2)	$\bar{T}_{sm}$ (°C)	*SEE* (°C)	η_c (%)		% error	η_s (%)		% error	η_{24hour} (%)		% error	$Q_{morning}$ (MJ)		% error
				Cal	Exp		Cal	Exp		Cal	Exp		Cal	Exp	
17/8/2002	11.2	31.1	0.10	34.8	43.3	-19.6	65.8	60.4	8.9	16.0	17.9	-10.6	8.9	9.3	-4.3
3/10/2002	20.7	41.2	0.10	38.8	39.9	-2.7	64.1	61.7	3.9	19.7	18.7	5.3	14.7	14.2	3.5
11/10/2002	25.2	41.9	0.12	36.2	37.1	-2.4	62.7	63.3	-0.9	16.4	16.7	-1.8	19.0	19.0	0
13/11/2002	18.7	38.3	0.10	38.9	36.1	7.7	63.8	60.7	5.1	19.2	17.5	9.7	14.6	13.1	11.4
15/11/2002	20.7	40.6	0.03	38.3	38.2	0.2	61.7	61.5	0.3	18.2	16.4	11.0	15.0	14.2	5.6

Note: $\bar{T}_{sm}$ = average value of the mean storage temperature, T_{sm}, throughout the experimental test, SEE = standard error of estimate of T_{sm}, % error = (Cal – Exp) / Exp x 100, η_c = daytime collecting efficiency, η_s = storage efficiency during the cool down period at night, η_{24hour} = system efficiency during 24 hours, $Q_{morning}$ = amount of energy stored in the storage tank before sunrise of the next morning.